1000-0569/2019/035(01)-0204-14 *Acta Petrologica Sinica* 岩石学报 doi: 10.18654/1000-0569/2019.01.16

幔源岩浆氧化还原状态及对岩浆矿床成矿的制约*

柏中杰[1] 钟宏[1,2] 朱维光[1]

BAI ZhongJie[1], ZHONG Hong[1,2] and ZHU WeiGuang[1]

1. 中国科学院地球化学研究所,矿床地球化学国家重点实验室,贵阳 550081
2. 中国科学院大学,北京 100049

1. *State Key Laboratory of Ore Deposit Geochemistry, Institute of Geochemistry, Chinese Academy of Sciences, Guiyang* 550081, *China*
2. *University of Chinese Academy of Sciences, Beijing* 100049, *China*

2018-09-21 收稿,2018-11-20 改回.

Bai ZJ, Zhong H and Zhu WG. 2019. Redox state of mantle-derived magma and constraints on the genesis of magmatic deposits. *Acta Petrologica Sinica*, 35(1):204-214, doi:10.18654/1000-0569/2019.01.16

Abstract The redox state of mantle-derived basaltic magma is one of the key thermodynamic parameters controlling many basic geological processes. Methods commonly used to estimate redox state of basaltic magmas and its source rocks include valence state of multivalent elements, partition coefficient of multivalent elements, chemical equilibrium of coexisting mineral pairs and whole-rock chemical ratios. With the rapid development of petrological experiments and the advances in analytical techniques, it is possible to accurately estimate the oxygen fugacity of mantle-derived basaltic magma and source rocks. This has greatly promoted the studies on composition of mantle source, evolutional history of partial melting, differentiation of mantle-derived basaltic magma, genesis of magmatic deposits, and metallogenic processes. The variable redox state of the mantle-derived magma is not only related to the tectonic settings, but also closely related to the mantle depth (pressure), metasomatism, and partial melting. Fractional crystallization, degassing and contamination of the magma can also change the oxygen fugacity of the magma in variable degrees at the shallow crust. Therefore, the mantle-derived magma exhibits variable oxygen fugacity even from the same geodynamic background. The oxygen fugacity of mantle-derived magma exerts critical controls on geochemical behavior of metals (e.g., PGE, Au, Cu) during partial melting of the source region, magma differentiation trends, relative saturation time of Fe-Ti-V oxide and its V content, and sulfur solubility in the magma. Thus, the ore-forming processes of Fe-Ti-V oxide deposits and Ni-Cu-(PGE) sulfide deposits are significantly influenced by the oxygen fugacity of magma.

Key words Redox state; Oxygen fugacity; Fe-Ti-V oxide deposit; Ni-Cu-PGE sulfide deposit

摘 要 岩浆的氧化还原状态是控制许多基本地质过程的关键热动力学参数之一。估算玄武质岩浆和源区岩石氧化还原状态的常用方法主要包括多价元素的价态、多价元素的分配系数、共存矿物对的化学平衡和全岩化学比值。岩石学实验的深入和分析技术手段的快速发展使精确估算岩浆氧逸度成为可能。这有力地促进了对地幔源区成分、岩浆的部分熔融程度和熔融方式与分异演化历史,以及岩浆矿床的成因机制及成矿过程的研究。幔源岩浆的氧化还原状态复杂多变,不仅与构造背景有关,还与地幔深度(压力)、交代作用和部分熔融有着密切联系。而在岩浆到达浅部地壳后,结晶分异、岩浆去气和同化混染等过程也能不同程度地改变岩浆的氧逸度。因此,即使来自同一构造背景的幔源岩浆也呈现出明显的氧逸度不均一性。氧逸度的高低对源区部分熔融过程中金属元素的地球化学行为、岩浆的分异演化趋势、Fe-Ti-V 氧化物饱和时间的早晚和 S 在岩浆中的溶解度具有明显的控制作用。因此,岩浆的氧逸度对钒钛磁铁矿矿床和汇聚板块边缘的岩浆硫化物矿床的成矿过程具有显著的影响。

关键词 氧化还原状态;氧逸度;钒钛磁铁矿矿床;岩浆硫化物矿床

---

* 本文受国家重点研发计划"深地资源开采"重点专项(2016YFC0600405)和国家自然科学基金项目(41425011、41873055、41473048)联合资助.

第一作者简介:柏中杰,男,1983,副研究员,矿床地球化学专业,E-mail: baizhongjie@vip.gyig.ac.cn

中图法分类号 P611.1

岩浆矿床是起源于地幔部分熔融的基性-超基性岩浆上侵到地壳后经历结晶分异、地壳混染、岩浆混合、液态不混溶等演化过程,进而发生成矿物质的分离和聚集而形成的矿床。其主要类型包括岩浆钒钛磁铁矿矿床、铬铁矿矿床以及岩浆硫化物矿床,是 V、Ti、Cr、Ni、PGE 等资源的主要来源(Lee,1996; Arndt *et al.*,2005; Cawthorn *et al.*,2005)。典型的岩浆硫化物矿床包括俄罗斯的 Nori'sk-Talnakh(Arndt *et al.*,2003)、加拿大的 Voisey'Bay(Ripley and Li,2011)、以及我国的金川和夏日哈木等(Li and Ripley,2011; Song *et al.*,2016)。而位于我国峨眉山大火成岩省内带的攀西地区则是世界著名的岩浆钒钛磁铁矿矿床聚集区(Zhong *et al.*,2002,2005; 徐义刚等,2013)。此外,南非 Bushveld 杂岩体不仅赋存有世界上最大的 PGE 矿床,同时还赋存有世界最大的铬铁矿矿床和钒钛磁铁矿矿床(Naldrett,2011; 王焰等,2017)。通常情况下,幔源岩浆侵入地壳形成的镁铁-超镁铁岩体主要由硅酸盐矿物组成,仅仅含有少量的氧化物和其它副矿物。地幔源区的物质组成、部分熔融的模式或程度、岩浆侵位和结晶的时间及机制、同化混染的地壳物质组成等都与成矿息息相关(Arndt *et al.*,2005)。地幔源区或幔源岩浆氧逸度是各种地质过程中的关键热动力学参数之一,在固体地球科学、全球气候变化以及生命起源等研究中都具有极为重要的作用(喻学惠,1990; 赖绍聪和周天祯,1993; 刘丛强等,2001)。在地幔源区部分熔融和岩浆结晶分异过程中,氧逸度的高低极大的控制了岩浆中 S 的溶解度,进而对上述过程中 PGE、Au、Cu、Ni 等金属元素的迁移和富集具有显著影响(Barnes and Lightfoot,2005; Naldrett,2011)。此外,岩浆氧逸度的高低不仅明显影响 Fe-Ti 氧化物中金属 V 的含量(Toplis and Corgne,2002),还对 Fe-Ti 氧化物在岩浆结晶分异过程中开始结晶时间的早晚有着决定性作用(Toplis and Carroll,1995),从而决定了岩浆是向富 Fe 贫 Si 的 Fenner 趋势演化(Fenner,1929)还是向富 Si 贫 Fe 的 Bowen 趋势演化(Bowen,1928)。因此,岩浆的氧逸度对钒钛磁铁矿矿床和岩浆硫化物矿床的成矿过程具有明显的控制作用(Mungall *et al.*,2006; Thakurta *et al.*,2008; Tomkins *et al.*,2012)。地幔源区或幔源岩浆氧逸度的高低与许多地质过程密切相关,不仅来自不同构造背景的岩浆氧逸度存在明显差异、还与地幔部分熔融时的深度(压力)、部分熔融程度和熔融方式、交代作用等有着密切联系(Ballhaus *et al.*,1990; Woodland *et al.*,1996; Woodland and Koch,2003; Gaetani,2016)。而结晶分异、地壳混染、岩浆去气等浅部地壳过程同样会改变岩浆的氧逸度(Carmichael and Ghiorso,1986; Thakurta *et al.*,2008; Moussallam *et al.*,2016)。近年来,实验岩石学和分析测试技术取得了长足进步和快速发展,特别是 LA-ICP-MS 与 X 射线吸收近边结构谱(μ-XANES)原位微区分析技术在地学研究中的应用日趋成熟。前者能够分析多价元素(如,V、Cr、Mn、Eu 等)的含量,而后者能够精确测定多价主(如 $Fe^{2+,3+}$)微量(如 $V^{2+,3+,4+,5+}$)元素不同价态比值。高质量的分析数据使准确获取幔源岩浆的氧化还原状态成为可能,进而为深入研究岩浆钒钛磁铁矿矿床和汇聚板块边缘的岩浆硫化物矿床成矿作用提供新的制约。本文在近年来国内外同行研究成果的基础上,尝试对幔源岩浆氧逸度的研究进展进行初步的总结和综述。

1 幔源岩浆及地幔源区氧逸度的估算方法

氧逸度计算方法主要包括:(1)多价主(如 $Fe^{2+,3+}$)、微量(如 $V^{2+,3+,4+,5+}$)元素不同价态比值;(2)多价元素在单矿物/与熔体间的分配系数;(3)全岩微量元素比值(如 V/Sc、Zn/Fe);(4)矿物化学平衡等。

(1)多价元素(如 Fe、V、Cr)不同价态比值:幔源玄武质熔体形成的火山玻璃或包裹于矿物中的熔融包裹体在成分上近似于岩浆成分,因此能够直接提供岩浆的氧逸度信息(Sutton *et al.*,2005; Cottrell *et al.*,2009)。经过适当的热力学校准,火山玻璃或熔融包裹体的多价元素不同价态比值能够直接用来计算玄武质熔体的氧逸度。基于一系列实验校准(Jayasuriya *et al.*,2004; Kress and Carmichael,1991; Putirka,2016),氧逸度与玄武质岩浆 $Fe^{3+}/\sum Fe$ 比值之间的关系可用以下公式表示:

$$ln\left(\frac{X_{Fe_2O_3}}{X_{FeO}}\right)=a\ln fO_2+\frac{b}{T}+c+\sum_i d_i X_i \qquad ①$$

其中 a、b、c 和 d_i 为实验常数。

传统分析 $Fe^{3+}/\sum Fe$ 比值的方法是采用湿化学分析(包括比色法)和使用穆斯堡尔谱。近年来,基于 μ-XANES 分析技术逐渐发展成熟,该分析技术能够对复杂样品在传统薄片上进行直接的非破坏性微尺度分析并获取元素的价态信息,并具有较高的精度和空间分辨率,因此被广泛用于测定地质样品特别是熔体包裹体中的 $Fe^{3+}/\sum Fe$ 比值并以此估算其氧逸度(Alderman *et al.*,2017; Cottrell *et al.*,2009; Crabtree and Lange,2012; Zhang *et al.*,2016)。由于仅需很低的元素含量(最小元素检测限为 10^{-6} 量级),μ-XANES 能获得很高的灵敏度,因此该方法也被广泛用于测定多价微量元素不同价态的比值,并以此来计算其氧逸度(Sutton *et al.*,2005; Balan *et al.*,2006; Head *et al.*,2018; Lanzirotti *et al.*,2018)。例如,Lanzirotti *et al.*(2018)使用 XANES 测定了 Kilauea 及 East Pacific Rise 玄武质玻璃中的 V 的价态,以此计算出的氧逸度值与采用 $Fe^{3+}/\sum Fe$ 比值计算获得的氧逸度值在误差范围内基本一致。

(2)多价元素矿物/熔体分配系数:不同价态微量元素在矿物/熔体之间的分配系数存在差异,其在矿物/熔体之间的分配系数与氧逸度呈明显的负相关关系(Canil,1997,

1999)。例如从 V^{3+} 到 V^{4+} 再到 V^{5+},其在矿物相中的相容性逐渐降低,因此 V 在矿物/熔体之间的分配系数随着氧逸度的升高而降低(Canil, 1997, 1999)。橄榄石是最早从玄武质岩浆中结晶出来的矿物,因此通过分析 V 等多价元素在橄榄石-熔体之间的分配系数更能反映原始岩浆的氧逸度(Canil, 1997; Gaetani and Grove, 1997; Mallmann and O'Neill, 2009, 2013)。Mallmann and O'Neill (2013) 给出的氧逸度与 $D_V^{Ol/melt}$ 之间的关系如下:

$$lg_fO_2(\Delta QFM) = -7.7 - \left(\frac{lgD_V^{Ol/melt}}{0.2639}\right) - \left\{\frac{[822 - 3328(1 - Mg_{\#}^{Ol})^2 + 5326X_{KO_{0.5}}^{melt} + 746(X_{CaO}^{melt} + X_{NaO_{0.5}}^{melt}) - 3254(X_{SiO_2}^{melt} + X_{AlO_{1.5}}^{melt})]}{0.2639T}\right\} \quad ②$$

其中温度 T 为开氏温度,熔体成分为摩尔分数。该公式针对的是高温(>1250℃)无水体系,适用的氧逸度范围为 QFM-4 ~ QFM +4。而最近 Shishkina *et al.* (2018) 则给出了含水玄武质岛弧岩浆的关系式:

$$\Delta QFM = -3.07^{+0.26}_{-0.29} lgD_V^{Ol/melt} - 3.34^{+0.49}_{-0.49} \quad ③$$

该公式适用于 QFM-2 ~ QFM + 3.2,温度≤1250℃,MgO < 12%,Na_2O < 4.0% 及 H_2O < 6.5% 的玄武质岩浆。

此外,多价元素在尖晶石/熔体(Righter *et al.*, 2006; Papike *et al.*, 2013; Wijbrans *et al.*, 2015)、辉石/熔体(Karner *et al.*, 2007, 2008; Papike *et al.*, 2016)之间的分配系数与氧逸度之间也存在着类似的关系(图 1)。Mn^{2+} 与 Mn^{3+} 在磷灰石/熔体之间的分配系数同样受到氧逸度的控制,因此磷灰石的 Mn 含量也被用来估算硅酸盐岩浆的氧逸度(Miles *et al.*, 2014)。然而 Marks *et al.* (2016) 指出磷灰石中的 Mn 含量还明显受到岩浆温度、熔体成分、及同时形成的其他富 Mn 矿物的影响。此外,一些多价稀土元素(如 Eu、Ce)在锆石与熔体间的分配系数也被广泛用于中酸性岩浆的氧逸度估算(Trail *et al.*, 2012; Smythe and Brenan, 2016)。

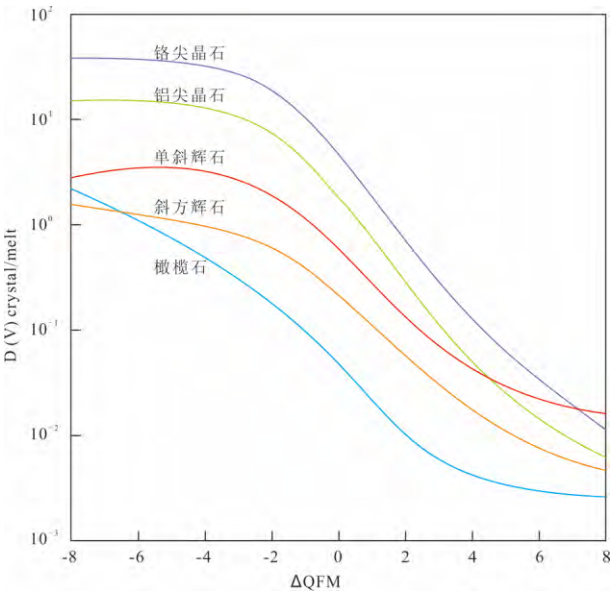

图 1 氧逸度对 V 在矿物和硅酸盐熔体之间的分配系数的影响(据 Mallmann and O'Neill, 2009)

Fig. 1 The effect of oxygen fugacity on the partitioning behaviour of V between crystals and silicate melt (after Mallmann and O'Neill, 2009)

(3) 全岩微量元素比值:由于多价元素 V 的分配系数与氧逸度密切相关这一特性,V 与在地幔部分熔融过程中地球化学行为相似的非氧化还原依赖元素(如 Sc、Ga、Y、Yb 等)之间的比值可以用来估算岩浆源区的氧化还原状态(Li and Lee, 2004; Lee *et al.*, 2005; Mallmann and O'Neill, 2009; Laubier *et al.*, 2014)。此外,在地幔部分熔融过程中 Fe^{2+} 与 Zn 具有相似的化学行为,而 Fe^{3+} 比 Fe^{2+} 更不相容,因此 Zn/Fe_T 比值也可以用来反映岩浆源区的氧逸度(Lee *et al.*, 2010)。Lee *et al.* (2005) 利用 V/Sc 比值估算出的 MORB 与 IAB 的源区具有相似的氧化还原状态,其氧逸度范围为 QFM-1.25 ~ +0.5。而 Laubier *et al.* (2014) 发现 V/Yb 比值从 MORB 到 BABB 到 IAB 逐渐升高,反映后者较前者源区更为氧化。V/Sc 等微量元素比值还不同程度受到矿物(如单斜辉石)分离结晶的影响,因此仅适用于演化程度较低(如 MgO > 8%)的幔源岩浆。

(4) 矿物化学平衡:处于化学平衡且没有重结晶或出溶的共生矿物组合成分常常被用来估算其结晶时的温度、压力及氧逸度。Fe-Ti 氧化物组合是最早被用来估算氧逸度的矿物对。磁铁矿-钛铁晶石固溶体与赤铁矿-钛铁矿固溶体之间的平衡对于温度和氧逸度非常敏感,因此可以用来同时估算 Fe-Ti 氧化物共生矿物对结晶或再平衡时的温度和氧逸度。根据实验结果,Buddington and Lindsley (1964) 首先给出了 Fe-Ti 氧化物的氧逸度估算方法。通过不断的改进,Ghiorso and Sack (1991) 给出了一套基于热动力学的氧逸度估算方法。Frost *et al.* (1988) 指出岩石的氧逸度不仅仅体现在 Fe-Ti 氧化物组合的成分上,同时体现在共存的硅酸盐矿物的成分上。Fe-Ti 氧化物与硅酸盐矿物之间存在以下平衡关系:SiO_2(石英) + $2Fe_2TiO_4$(钛铁晶石) = $2FeTiO_3$(钛铁矿) + Fe_2SiO_4(铁橄榄石),缩写为 QUILF。在此基础上,Lindsley and Frost (1992) 给出了一个估算氧逸度的 QUILF 电脑程序。镁铁-超镁铁质岩体在结晶之后的冷却过程中,磁铁矿与钛铁矿之间以及 Fe-Ti 氧化物与镁铁硅酸盐矿物之间将发生复杂的再平衡,而 Fe-Ti 氧化物自身也将经历亚固相出溶(Buddington and Lindsley, 1964; Frost *et al.*, 1988; Frost and Lindsley, 1992)。因此对于镁铁-超镁铁侵入岩,该计算方法获得的是磁铁矿-钛铁矿处于亚固相化学再平衡时的温度和氧逸度。岩石中各共生矿物通常具有不同的 Fe^{3+}/Fe^{2+} 比值,因此可以用来估算矿物化学平衡时的氧逸度。对于地幔

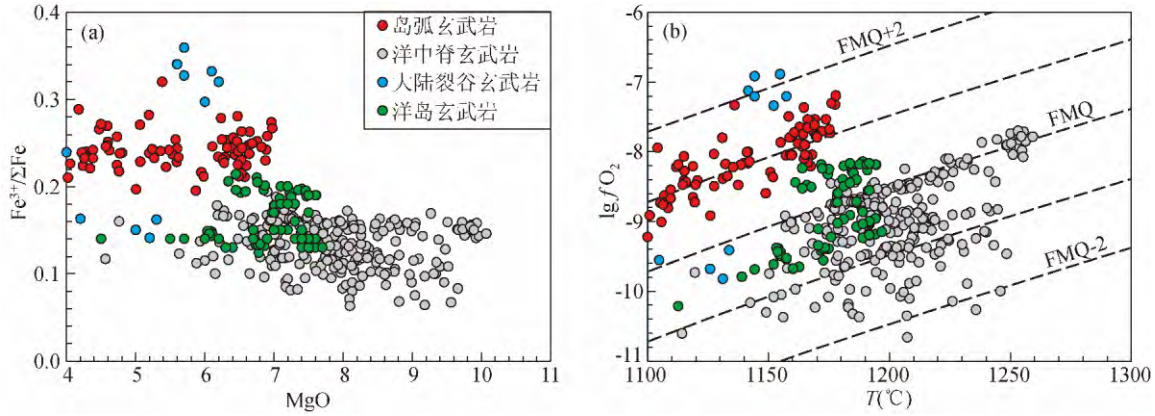

图 2　来自不同构造背景的玄武质岩浆的 $Fe^{3+}/\sum Fe$ 比值(a)及氧逸度(b)

f_{O_2} 与 T 计算方法采用 Jayasuriya *et al.* (2004，公式 12) 和 Putirka (2008，公式 13)．数据来源: 洋中脊玄武岩: Bézos and Humler (2005)，Cottrell and Kelley (2011)，Berry *et al.* (2018)；洋岛玄武岩: Moussallam *et al.* (2016)，Brounce *et al.* (2017)；岛弧玄武岩: Kelley and Cottrell (2012)，Brounce *et al.* (2014)

Fig. 2　The $Fe^{3+}/\sum Fe$ ratios (a) and oxygen fugacity (b) of basaltic magma from different geological settings

f_{O_2} and T is calculated using the methods outlined by Jayasuriya *et al.* (2004, Eq. 12) and Putirka, (2008, Eq. 13). Data sources: MORB: Bézos and Humler (2005), Cottrell and Kelley (2011), Berry *et al.* (2018); OIB: Moussallam *et al.* (2016), Brounce *et al.* (2017); ARC: Kelley and Cottrell. (2012), Brounce *et al.* (2014)

橄榄岩，最常见的矿物组合橄榄石-斜方辉石-尖晶石被用来估算氧逸度(O'Neill and Wall，1987; Wood，1991; Ballhaus *et al.*，1991)。Ballhaus *et al.* (1991) 给出了以下计算公式:

$$lgfO_2(\Delta QFM) = 0.27 + \frac{2505}{T} - \frac{400P}{T} - 6lg(X_{Fe}^{olv}) - \frac{3200(1-X_{Fe}^{olv})^2}{T} + 2lg(X_{Fe^{2+}}^{sp}) + 4lg(X_{Fe^{3+}}^{sp}) + 2630(X_{Al}^{sp})^2/T \quad ④$$

其中压力 P 和温度 T 为 GPa 和 K，$X_{Fe^{3+}}^{sp}$ 和 X_{Al}^{sp} 为尖晶石 $Fe^{3+}/\sum Fe$ 和 $Al/\sum R^{3+}$ 比值，X_{Fe}^{olv} 和 $X_{Fe^{2+}}^{sp}$ 分别为橄榄石和尖晶石的 $Fe^{2+}/(Fe^{2+}+Mg)$ 比值。该计算公式也被用来计算玄武岩和镁铁-超镁铁侵入岩的岩浆氧逸度。

2　地幔源区及幔源岩浆氧逸度高低及其控制因素

幔源岩浆的氧化还原状态继承自地幔源区并可能受到后期诸如结晶分异、岩浆去气和地壳混染等浅部过程的改变(Carmichael，1991; Kress and Carmichael，1991; Lee *et al.*，2005; Mallmann and O'Neill，2009; Kelley and Cottrell，2012; Grocke *et al.*，2016; Moussallam *et al.*，2016)。不同构造背景下地幔源区的氧化还原状态呈现出高度的不均一性(Ballhaus *et al.*，1990; Ballhaus，1993; Foley，2011; Gaillard *et al.*，2015)。橄榄石-斜方辉石-尖晶石化学平衡氧逸度计算结果表明: 大部分玄武质岩浆氧逸度范围为 FMQ-2 到 FMQ+3(Ballhaus *et al.*，1990，1991; Ballhaus，1993)，其中大洋中脊玄武岩(MORB)的氧逸度范围大约为 FMQ-2 ~ FMQ，而洋岛玄武岩(OIB)稍微氧化，其氧逸度范围大约为 FMQ ~ FMQ+2。高氧化的岩浆则来自于岛弧玄武岩(IAB)，其氧逸度范围为 FMQ+1 ~ FMQ+3。我们对近年来发表的(Bézos and Humler，2005; Cottrell and Kelley，2011; Kelley and Cottrell，2012; Brounce *et al.*，2014，2017; Moussallam *et al.*，2016; Berry *et al.*，2018)来自不同构造背景的玄武岩熔体包裹体的 $Fe^{3+}/\sum Fe$ 数据采用公式①进行了氧逸度计算。这些数据主要通过穆斯堡尔谱或 XANES 分析方法获得，能够更加准确反映岩浆的氧逸度。结果表明，MORB 的 $Fe^{3+}/\sum Fe$ 比值小于 0.18，其对应的氧逸度为范围为 QFM-2-QFM，夏威夷洋岛玄武岩的 $Fe^{3+}/\sum Fe < 0.22$，氧逸度为 QFM-QFM+1，马里亚纳岛弧玄武岩 $Fe^{3+}/\sum Fe$ 比值在 0.2 ~ 0.3 之间，对应的氧逸度为 QFM-QFM+2(图 2)。这些结果总体上与基于橄榄石-斜方辉石-尖晶石化学平衡所获得的结果基本一致。

氧逸度的差异不仅存在于不同的构造背景下，来源于同一构造背景下的岩浆同样呈现出氧逸度的不均一性。例如，夏威夷洋岛玄武岩(MgO > 8%)具有宽泛的 V/Sc(7 ~ 15)和 V/Yb(110 ~ 210)比值(图 3)，暗示其源区氧逸度变化范围约为 QFM-1 ~ QFM+1。Dixon *et al.* (1997)发现夏威夷玄武岩的 $Fe^{3+}/\sum Fe$ 比值与不相容元素呈正相关，认为小程度部分熔融形成的碱性玄武岩具有较高的氧逸度(FMQ+0.7)，随着部分熔融程度的加大而降低到 FMQ-0.8。在部分熔融过程中，Fe^{3+} 倾向于进入熔体而 Fe^{2+} 倾向于保留在固体之中。因此，经历小程度部分熔融形成的碱性玄武岩往往具有较高的氧逸度(最高可达 FMQ+2.5)(Carmichael，1991; Mungall *et al.*，2006; Moussallam *et al.*，2014)。Gaetani

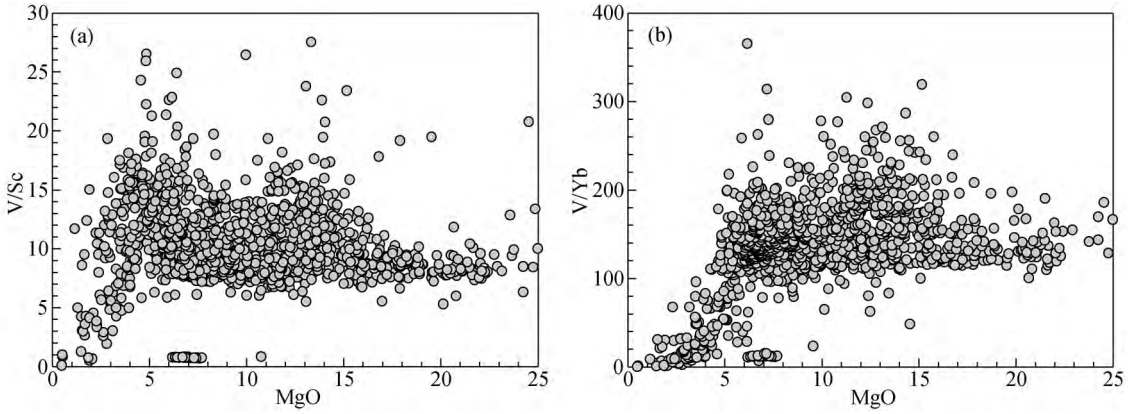

图3 夏威夷玄武岩的 V/Sc (a) 与 V/Yb (b) 比值对 MgO

宽泛的 V/Sc(7~15) 和 V/Yb(110~210) 比值反映其源区具有变化的氧逸度. 数据来源: http://georoc.mpch-mainz.gwdg.de/georoc/Entry.html

Fig. 3 The plots of V/Sc (a) and V/Yb (b) ratios against MgO of the Hawaiian basalt

The variation of V/Sc (7~15) and V/Yb (110~210) ratios indicates that heterogeneous oxygen fugacity occur in the mantle source region. Data resources: http://georoc.mpch-mainz.gwdg.de/georoc/Entry.html

(2016) 指出,氧逸度的变化与部分熔融程度和熔融方式都存在密切关系。在等压批式部分熔融过程中,熔体的 $Fe^{3+}/\sum Fe$ 比值及相应的氧逸度随着熔融程度的增加而升高;相反,在绝热减压批式部分熔融过程中,熔体的 $Fe^{3+}/\sum Fe$ 比值及相应的氧逸度随着熔融程度的增加而降低(Gaetani, 2016)。

氧逸度的变化还与地幔深度(压力)和交代作用有着密切联系。由于压力对石榴石 Fe^{2+}-Fe^{3+} 平衡的影响(Wood *et al.*, 1990),随着地幔深度的增加,地幔橄榄岩的氧逸度逐渐降低(Woodland and Koch, 2003; McCammon and Kopylova, 2004; Lazarov *et al.*, 2009; Goncharov *et al.*, 2012)。来自 Kaapvaal 克拉通岩石圈地幔包体的研究表明,深度从 80 到 220 公里的橄榄岩包体的氧逸度降低了约 3 个 log 单位(从 QFM-1 到 QFM-4, Woodland and Koch, 2003)。与此类似,Siberian 克拉通岩石圈地幔的氧逸度从顶部的 QFM+1 降低到底部的 QFM-4 (Goncharov *et al.*, 2012)。一些板内岩浆的氧化特征可能与玄武质岩浆产生之前富 CO_2 和 H_2O 熔体的交代作用有关(Woodland *et al.*, 1996; McCammon *et al.*, 2001; Creighton *et al.*, 2008)。从未发生交代的橄榄岩到弱交代的橄榄岩再到强交代的橄榄岩,伴随着尖晶石 Cr/(Cr+Al) 的增加,其氧逸度从 QFM-1 逐渐升高到 QFM+1 (Ballhaus *et al.*, 1991)。岛弧岩浆具有比 MORB 更高的氧逸度,部分学者认为这是来自俯冲板片的氧化性流体交代岛弧地幔源区所导致(Wood *et al.*, 1990; Brandon and Draper, 1996; Evans *et al.*, 2012; Brounce *et al.*, 2014)。

在岩浆到达浅部地壳后,橄榄石、辉石、磁铁矿等矿物的结晶分异将改变岩浆的 Fe^{3+}/Fe_{Tot} 比值,从而改变岩浆的氧逸度(Carmichael and Ghiorso, 1986)。最近研究表明,岩浆的 $Fe^{3+}/\sum Fe$ 比值在橄榄石、辉石结晶分异过程中变化不大,并不会明显改变岩浆的氧逸度(Cottrell and Kelley, 2011; Crabtree and Lange, 2012; Kelley and Cottrell, 2012)。相反,磁铁矿的结晶将显著降低岩浆的氧逸度。例如 MORB 岩浆经过 14% 的橄榄石结晶,岩浆的 $Fe^{3+}/\sum Fe$ 仅仅增加了 0.025(Cottrell and Kelley, 2011)。Kiglapait 侵入体母岩浆经历了高达 93.5% 的结晶分异(温度从 1254℃ 降低到 1054℃),其氧逸度从初始的约 QFM-0.4 缓慢升高到约 QFM+0.6;而当磁铁矿饱和结晶后(温度降低到 1033℃),其氧逸度迅速降低到 QFM-0.4(Morse, 2015)。而 Skaergaard 侵入体的氧逸度从磁铁矿开始饱和时的 QFM 持续降低到岩浆演化晚期的 QFM-2(Frost and Lindsley, 1992)。岩浆的去气作用同样可能改变岩浆的氧逸度(Carmichael and Ghiorso, 1986; Carmichael, 1991; Kelley and Cottrell, 2012; Moussallam *et al.*, 2016)。夏威夷玄武岩的 $Fe^{3+}/\sum Fe$ 比值随着 H_2O 和 S 含量的逐渐降低而降低,反映其氧逸度在岩浆去气过程中从 QFM+1 降低到 QFM-0.4(Brounce *et al.*, 2017)。玄武质岩浆同化混染氧化性或还原性地层将明显改变岩浆的氧逸度。如俄罗斯侵入含煤沉积地层中的 Siberian Traps 的玄武岩中含有大量的自然铁,其氧逸度可低达 FMQ-6(Iacono-Marziano *et al.*, 2012)。由岛弧岩浆形成的 Duke Island 杂岩体赋存有岩浆硫化物矿床,其硫化物饱和熔离被认为是氧化性的岛弧岩浆同化混染了还原性的碳质围岩所导致(Thakurta *et al.*, 2008)。相反,Ganino *et al.* (2008, 2013) 认为攀枝花钒钛磁铁矿矿床的母岩浆同化混染碳酸盐围岩导致氧逸度升高,进而使磁铁矿在岩浆演化的较早阶段结晶。

3 氧逸度对成矿过程的影响

3.1 钒钛磁铁矿矿床

拉斑玄武质岩浆在结晶分异过程中既可以朝着逐渐富

Si 贫 Fe 的 Bowen 分异趋势演化(Bowen, 1928),也可以朝着逐渐富 Fe 贫 Si 的 Fenner 分异趋势演化(Fenner, 1929)。Fe-Ti-V 氧化物从岩浆中结晶出来的时间决定了岩浆的分异演化会遵循哪种分异趋势。在 Fe-Ti-V 氧化物达到饱和之前,结晶出的硅酸盐矿物组合通常相对岩浆具有较低的 FeO 含量,从而使得岩浆向富 Fe 的方向演化;而当 Fe-Ti-V 氧化物达到饱和之后,结晶出的矿物组合具有相对岩浆更高的 FeO 含量,从而改变岩浆的分异趋势。如在南非 Bushveld 杂岩体和加拿大 Kiglapait 侵入体中,残余岩浆的 FeO 含量在磁铁矿达到饱和之后就逐渐降低(Morse, 1981; Tegner and Cawthorn, 2010)。Toplis and Carroll (1995) 的实验岩石学研究表明,在玄武质岩浆体系中,氧逸度的变化对 Fe-Ti-V 氧化物的结晶时间起着明显的控制作用。氧逸度的升高会扩大玄武质岩浆体系中磁铁矿的稳定范围,导致磁铁矿提早从岩浆中结晶出来。与磁铁矿饱和受控于岩浆氧逸度不同,钛铁矿的饱和结晶则主要决定于岩浆中的 TiO_2 含量(Toplis and Carroll, 1995)。因此,岩浆氧逸度的高低对钒钛磁铁矿矿床成矿的影响主要体现在以下方面: ①矿床成矿时间: 如前所述,氧逸度的高低极大地影响磁铁矿在岩浆演化过程中饱和时间的早晚,从而决定矿床是在岩浆演化的早期还是晚期成矿; ②金属矿物组合: 当岩浆具有较高的氧逸度时,磁铁矿在岩浆演化的较早阶段开始结晶。此时由于岩浆中 TiO_2 含量较低而未能使钛铁矿达到饱和。形成以钒钛磁铁矿为主的金属矿物组合。如我国著名的攀枝花矿床,其最重要的下部含矿带中的矿石主要由钒钛磁铁矿矿物组成(Pang *et al.*, 2008)。相反,较低的氧逸度会推迟磁铁矿的结晶,使岩浆沿 Fenner 趋势演化而逐渐富 Fe 和 Ti。最终钒钛磁铁矿和钛铁矿同时从岩浆中结晶出来,形成以钒钛磁铁矿和钛铁矿共生的金属矿物组合; ③磁铁矿中的 V 含量: V 在磁铁矿与岩浆中的分配系数与岩浆的氧逸度呈负相关关系(Toplis and Corgne, 2002)。因此结晶于较低氧逸度下的磁铁矿往往具有较高的 V 含量。例如 Bushveld 杂岩体的母岩浆具有较低的氧逸度(NNO ~ NNO-1; Toplis and Corgne, 2002),结晶的磁铁矿中 V 含量可高达 12000×10^{-6}(Molyneux, 1974)。相反,结晶于较高氧逸度下的攀枝花矿床的磁铁矿的 V 含量仅有约 5000×10^{-6}(Pang *et al.*, 2008; Song *et al.*, 2013)。④岩浆液态不混溶: 岩浆液态不混溶常常被用来解释钒钛磁铁矿矿床的成因。氧逸度对岩浆液态不混溶的影响非常复杂,氧逸度升高将导致高的 Fe^{3+}/Fe^{2+} 比值,从而扩宽液态不混溶区域(immiscibility field)并增加液态不混溶发生的温度上限(Naslund, 1983; Philpotts and Doyle, 1983)。另一方面,氧逸度的升高会导致 Fe-Ti 氧化物的提前饱和,使岩浆朝着富 Si 贫 Fe 的 Bowen 分异趋势演化,从而抑制岩浆液态不混溶的发生(Philpotts and Doyle, 1983)。Philpotts and Doyle (1983) 的部分熔融实验结果显示,玄武质岩浆在低于 1018℃和 MW 和 FMQ 氧逸度下发生了液态不混溶,而当氧逸度升高到 NNO 时,大量的磁铁矿结晶,液态不混溶终止。

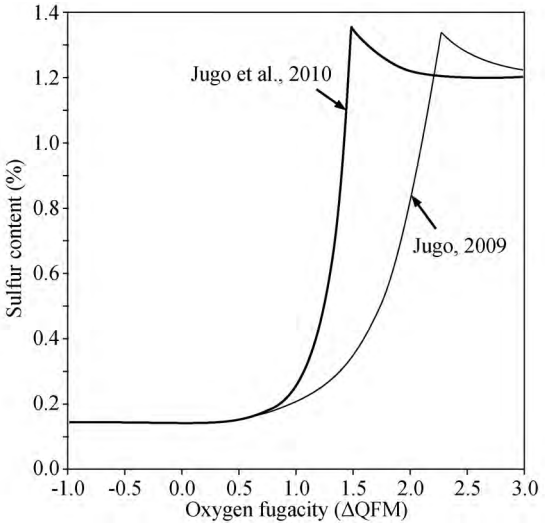

图 4 不同氧逸度下硫化物及石膏饱和时岩浆中的 S 含量(据 Jugo *et al.*, 2010)

随着氧逸度从 QFM 升高到 QFM + 2,岩浆中 S 的溶解度增加了约一个数量级

Fig. 4 The sulfur content at sulfide and anhydrite saturation at different oxygen fugacity (after Jugo *et al.*, 2010)

The solubility of Sulfur in magma increased by about an order of magnitude with the increase of oxygen fugacity from QFM to QFM + 2

3.2 岩浆硫化物矿床

S 在低氧逸度(< FMQ)和高氧逸度(> FMQ + 2)下分别以硫化物(S^{2-})和硫酸盐(S^{6+})的形式存在于玄武质岩浆中(Jugo, 2009; Jugo *et al.*, 2010)。后者在玄武质岩浆中的溶解度较前者高出一个数量级(图 4)。而当氧逸度范围位于 FMQ ~ FMQ + 2 的过渡区间时,S 同时以 S^{2-} 和 S^{6+} 存在。随着氧逸度的升高,S^{6+}/S^{2-} 比值增大,因此 S 在岩浆中的溶解度也随之升高(Jugo, 2009; Jugo *et al.*, 2010)。由于在硫化物熔体与硅酸盐岩浆之间极高的分配系数(PGE: $10^4 \sim 10^5$, Au: $10^3 \sim 10^4$, Cu: $10^2 \sim 10^3$; Naldrett, 2011 及其参考文献),PGE、Au、Cu 等亲硫元素将主要进入硫化物熔体中。因此,在部分熔融过程中,若硫化物残留在地幔将使部分熔融形成的玄武质熔体亏损上述金属元素。地幔中 S 含量大约为 250×10^{-6}(Palme and O'Neill, 2004),在氧逸度较低的情况下(如 < FMQ)只有较高程度的部分熔融(如 25%; Keays, 1995)才能耗尽地幔中的硫化物,产生的岩浆才有利于形成岩浆硫化物矿床。而当氧逸度较高时,仅需要很小的部分熔融程度即可将硫化物耗尽并将 PGE、Au、Cu 等亲硫元素转移到岩浆中。此时岩浆中的亲硫元素(如 PGE、Au 等)含量将明显高于低氧逸度下高程度部分熔融形成的岩浆(图 5)。例如,夏威夷碱性玄武岩被认为是在高氧逸度下通过低程度部分熔融形成,其 Au 含量可高达 36×10^{-9}(Sisson, 2003)。西伯利亚地区二叠纪的麦美奇岩和碱性苦橄岩是目前已知的由软流圈低程度部分熔融形成的最典型例子。Mungall *et*

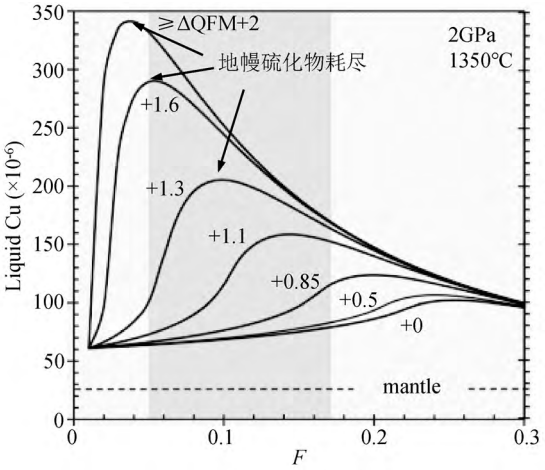

图5 不同氧逸度和部分熔融程度下地幔橄榄岩部分熔融形成的熔体的Cu含量(据Lee *et al.*, 2012)

Fig. 5 Cu contents during partial melting of mantle peridotite under different oxygen fugacity and degree of partial melting (after Lee *et al.*, 2012)

al. (2006)观察到麦美奇岩和碱性苦橄岩含有很高的PGE含量,表明其源区无硫化物残留,这与岩浆较高的氧逸度(QFM+2.5)特征一致。

硫(S)在岩浆中的溶解度主要受到温度、压力、氧逸度及岩浆成分的影响(Naldrett, 2011)。一般认为,在结晶分异过程中,S在高氧逸度的玄武质岩浆中具有非常高的溶解度,硫化物饱和被推迟、甚至不能达到饱和,从而使Cu、Au等元素逐渐富集到残余熔体中并最终形成斑岩型或其它热液型Cu-Au矿床(Sun *et al.*, 2004; Park *et al.*, 2015; Hao *et al.*, 2017)。相反,S更容易在低氧逸度的玄武质岩浆中达到饱和从而发生硫化物熔离并形成岩浆硫化物矿床。事实上,低氧逸度的玄武质岩浆通常含有约1000×10^{-6}的S,其至少要经过40%以上的结晶分异才能使岩浆中的S达到饱和,此时岩浆中的Ni已经被橄榄石消耗殆尽(Barnes and Lightfoot, 2005)。在结晶分异过程中,氧逸度的改变并不能明显降低S的溶解度,地壳混染导致S的溶解度的降低或外源S的加入才是促使S在岩浆演化的早期阶段达到饱和的主要因素。然而S在氧化性的玄武质岩浆中通常具有非常高的溶解度。西伯利亚二叠纪高氧逸度的碱性玄武岩部分熔融程度<7%(Mungall *et al.*, 2006),岩浆中S含量将高达3500×10^{-6}。而俯冲交代的地幔楔比其他地幔源区具有更高的S含量(de Hoog *et al.*, 2001),部分熔融形成的岛弧玄武岩S的含量可高达$5000\times10^{-6}\sim6000\times10^{-6}$(Vigouroux *et al.*, 2008; Rowe *et al.*, 2009)。此时岩浆氧逸度的降低将迅速降低岩浆中S的溶解度,从而发生硫化物或硫酸盐饱和(图4)。例如,在形成Duke Island杂岩体过程中高氧逸度的岛弧岩浆同化混染了还原性的碳质围岩,导致氧逸度的降低及S饱和,并形成岩浆硫化物矿床(Thakurta *et al.*, 2008)。

4 结论与展望

分析测试技术的发展为岩浆氧逸度的精确估算提供了有力支撑。近年来,幔源岩浆氧逸度的研究促进了对地幔源区成分、岩浆的部分熔融与分异演化历史和矿床的成矿过程的深入了解,为研究矿床成因提供了新的约束。然而,不同的估算方法得出的氧逸度存在一定差异,例如岛弧玄武岩与洋中脊玄武岩的V/Sc比值显示两者的源区可能具有相似的氧逸度(Lee *et al.*, 2005)。而通过橄榄石-斜方辉石-尖晶石组合及$Fe^{3+}/\sum Fe$比值估算的氧逸度表明岛弧玄武岩的氧逸度明显高于洋中脊玄武岩(Ballhaus *et al.*, 1991; Brounce *et al.*, 2014; Kelley and Cottrell, 2012)。目前导致这种差异的原因尚不明确。$Fe^{3+}/\sum Fe$比值与矿物化学平衡反映的是岩浆或矿物相最后平衡时的氧化还原状态。而当岩浆离开源区后,结晶分异、地壳混染、岩浆去气等浅部过程将不同程度地改变岩浆的氧逸度。不同方法估算出的氧逸度差异可能反映的是岩浆在部分熔融与分异演化过程的不同阶段的氧逸度变化。另一种可能是不同估算方法本身误差所致。因此,运用不同的方法针对未明显遭受浅部地质过程影响的地质样品(如富含挥发分的苦橄岩样品)进行氧逸度估算有助于评估各方法估算结果的差异及其原因。此外,基于$Fe^{3+}/\sum Fe$比值和橄榄石V分配系数的氧逸度估算公式中并不包含压力参数,在实验校准过程中并没有考虑压力对多价元素价态及分配系数的影响。最近的研究表明,在氧逸度不变的情况下,$Fe^{3+}/\sum Fe$比值随着压力的增加而逐渐降低(O'Neill *et al.*, 2006; Zhang *et al.*, 2017)。压力变化似乎同样会改变岩浆中$S^{6+}/\sum S$比值。传统观点认为,当氧逸度高于QFM+2时,S在岩浆中以S^{6+}形式存在,因而具有极高的溶解度(Jugo, 2009; Jugo *et al.*, 2010)。需要指出的是,这一结果是基于0.2GPa压力下的实验研究所获得。最近(Matjuschkin *et al.*, 2016)的实验结果显示,当压力增加到1.0GPa,在氧逸度为QFM+2时S仍主要以S^{2-}的形式存在,直到氧逸度提高到NNO+3时,S才全部以S^{6+}的形式存在。如果这一实验结果正确,则意味着岛弧岩浆中S在地幔源区或下地壳深部岩浆房主要以S^{2-}存在,其在岩浆中的溶解度将远远低于传统认知。显然,这将极大地改变对与岛弧岩浆有关的岩浆硫化物矿床和斑岩-浅成低温热液型Cu-Au矿床成因的认识。因此,压力变化对元素价态的影响需要进一步深入研究。

致谢 感谢胡瑞忠研究员邀请撰写该篇综述论文;感谢两位评审人在审稿过程中提出的宝贵意见。

谨以此文庆贺叶大年先生八十华诞。

References

Alderman OLG, Wilding MC, Tamalonis A, Sendelbach S, Heald SM, Benmore CJ, Johnson CE, Johnson JA, Hah HY and Weber JKR. 2017. Iron K-edge X-ray absorption near-edge structure spectroscopy of aerodynamically levitated silicate melts and glasses. Chemical Geology, 453: 169 – 185

Arndt NT, Czamanske GK, Walker RJ, Chauvel C and Fedorenko VA. 2003. Geochemistry and origin of the intrusive hosts of the Noril'sk-Talnakh Cu-Ni-PGE sulfide deposits. Economic Geology, 98(3): 495 – 515

Arndt NT, Lesher CM and Czamanske GK. 2005. Mantle-derived magmas and magmatic Ni-Cu-(PGE) deposits. In: Hedenquist JW, Thompson JFH, Goldfarb RJ and Richards JP (eds.). Economic Geology 100th Anniversary Volume. Littleton: Society of Economic Geologists, 5 – 23

Balan E, De Villiers JPR, Eeckhout SG, Glatzel P, Toplis MJ, Fritsch E, Allard T, Galoisy L and Calas G. 2006. The oxidation state of vanadium in titanomagnetite from layered basic intrusions. American Mineralogist, 91(5 – 6): 953 – 956

Ballhaus C, Berry RF and Green DH. 1990. Oxygen fugacity controls in the Earth's upper mantle. Nature, 348(6300): 437 – 440

Ballhaus C, Berry RF and Green DH. 1991. High pressure experimental calibration of the olivine-orthopyroxene-spinel oxygen geobarometer: Implications for the oxidation state of the upper mantle. Contributions to Mineralogy and Petrology, 107(1): 27 – 40

Ballhaus C. 1993. Redox states of lithospheric and asthenospheric upper mantle. Contributions to Mineralogy and Petrology, 114(3): 331 – 348

Barnes SJ and Lightfoot PC. 2005. Formation of magmatic nickel-sulfide ore deposits and processes affecting their copper and platinum-group element contents. In: Hedenquist JW, Thompson JFH, Goldfarb RJ and Richards JP (eds.). Economic Geology 100th Anniversary Volume. Littleton: Society of Economic Geologists, 179 – 214

Berry AJ, Stewart GA, O'Neill HSC, Mallmann G and Mosselmans JFW. 2018. A re-assessment of the oxidation state of iron in MORB glasses. Earth and Planetary Science Letters, 483: 114 – 123

Bézos A and Humler E. 2005. The $Fe^{3+}/\sum Fe$ ratios of MORB glasses and their implications for mantle melting. Geochimica et Cosmochimica Acta, 69(3): 711 – 725

Bowen NL. 1928. The Evolution of the Igneous Rocks. Princeton: Princeton University Press

Brandon AD and Draper DS. 1996. Constraints on the origin of the oxidation state of mantle overlying subduction zones: An example from Simcoe, Washington, USA. Geochimica et Cosmochimica Acta, 60(10): 1739 – 1749

Brounce M, Stolper E and Eiler J. 2017. Redox variations in Mauna Kea lavas, the oxygen fugacity of the Hawaiian plume, and the role of volcanic gases in Earth's oxygenation. Proceedings of the National Academy of Sciences of the United States of America, 114(34): 8997 – 9002

Brounce MN, Kelley KA and Cottrell E. 2014. Variations in $Fe^{3+}/\sum Fe$ of mariana arc basalts and mantle wedge f_{O_2}. Journal of Petrology, 55(12): 2513 – 2536

Buddington AF and Lindsley DH. 1964. Iron-titanium oxide minerals and synthetic equivalents. Journal of Petrology, 5(2): 310 – 357

Canil D. 1997. Vanadium partitioning and the oxidation state of Archaean komatiite magmas. Nature, 389(6653): 842 – 845

Canil D. 1999. Vanadium partitioning between orthopyroxene, spinel and silicate melt and the redox states of mantle source regions for primary magmas. Geochimica et Cosmochimica Acta, 63(3 – 4): 557 – 572

Carmichael ISE and Ghiorso MS. 1986. Oxidation-reduction relations in basic magma: A case for homogeneous equilibria. Earth and Planetary Science Letters, 78(2 – 3): 200 – 210

Carmichael ISE. 1991. The redox states of basic and silicic magmas: A reflection of their source regions? Contributions to Mineralogy and Petrology, 106(2): 129 – 141

Cawthorn RG, Barnes SJ, Ballhaus C and Malitch K. 2005. Platinum group element, chromium, and vanadium deposits in mafic and ultramafic rocks. In: Hedenquist JW, Thompson JFH, Goldfarb RJ and Richards JP (eds.). Economic Geology 100th Anniversary Volume. Littleton: Society of Economic Geologists, 215 – 249

Cottrell E, Kelley KA, Lanzirotti A and Fischer RA. 2009. High-precision determination of iron oxidation state in silicate glasses using XANES. Chemical Geology, 268(3 – 4): 167 – 179

Cottrell E and Kelley KA. 2011. The oxidation state of Fe in MORB glasses and the oxygen fugacity of the upper mantle. Earth and Planetary Science Letters, 305(3 – 4): 270 – 282

Crabtree SM and Lange RA. 2012. An evaluation of the effect of degassing on the oxidation state of hydrous andesite and dacite magmas: A comparison of pre- and post-eruptive Fe^{2+} concentrations. Contributions to Mineralogy and Petrology, 163(2): 209 – 224

Creighton S, Stachel T, Matveev S, Höfer H, McCammon C and Luth RW. 2008. Oxidation of the Kaapvaal lithospheric mantle driven by metasomatism. Contributions to Mineralogy and Petrology, 157(4): 491 – 504

de Hoog JCM, Mason PRD and van Bergen MJ. 2001. Sulfur and chalcophile elements in subduction zones: Constraints from a laser ablation ICP-MS study of melt inclusions from Galunggung Volcano, Indonesia. Geochimica et Cosmochimica Acta, 65(18): 3147 – 3164

Dixon JE, Clague DA, Wallace P and Poreda R. 1997. Volatiles in alkalic basalts form the North arch volcanic field, Hawaii: Extensive degassing of deep submarine-erupted alkalic series lavas. Journal of Petrology, 38(7): 911 – 939

Evans KA, Elburg MA and Kamenetsky VS. 2012. Oxidation state of subarc mantle. Geology, 40(9): 783 – 786

Fenner CN. 1929. The crystallization of basalts. American Journal of Science, 18(105): 225 – 253

Foley SF. 2011. A reappraisal of redox melting in the earth's mantle as a function of tectonic setting and time. Journal of Petrology, 52(7 – 8): 1363 – 1391

Frost BR, Lindsley DH and Andersen DJ. 1988. Fe-Ti oxide-silicate equilibrium: Assemblages with fayalitic olivine. American Mineralogist, 73(7 – 8): 727 – 740

Frost BR and Lindsley DH. 1992. Equilibria among Fe-Ti oxides, pyroxenes, olivine, and quartz: Part Ⅱ. Application. American Mineralogist, 77(9 – 10): 1004 – 1020

Gaetani GA and Grove TL. 1997. Partitioning of moderately siderophile elements among olivine, silicate melt, and sulfide melt: Constraints on core formation in the Earth and Mars. Geochimica et Cosmochimica Acta, 61(9): 1829 – 1846

Gaetani GA. 2016. The behavior of $Fe^{3+}/\sum Fe$ during partial melting of spinel lherzolite. Geochimica et Cosmochimica Acta, 185: 64 – 77

Gaillard F, Scaillet B, Pichavant M and Iacono-Marziano G. 2015. The redox geodynamics linking basalts and their mantle sources through space and time. Chemical Geology, 418: 217 – 233

Ganino C, Arndt NT, Zhou MF, Gaillard F and Chauvel C. 2008. Interaction of magma with sedimentary wall rock and magnetite ore genesis in the Panzhihua mafic intrusion, SW China. Mineralium Deposita, 43(6): 677 – 694

Ganino C, Harris C, Arndt NT, Prevec SA and Howarth GH. 2013. Assimilation of carbonate country rock by the parent magma of the Panzhihua Fe-Ti-V deposit (SW China): Evidence from stable isotopes. Geoscience Frontiers, 4(5): 547 – 554

Ghiorso MS and Sack O. 1991. Fe-Ti oxide geothermometry: Thermodynamic formulation and the estimation of intensive variables in silicic magmas. Contributions to Mineralogy and Petrology, 108(4): 485 – 510

Goncharov AG, Ionov DA, Doucet LS and Pokhilenko LN. 2012. Thermal state, oxygen fugacity and C-O-H fluid speciation in cratonic lithospheric mantle: New data on peridotite xenoliths from

the Udachnaya kimberlite, Siberia. Earth and Planetary Science Letters, 357 – 358: 99 – 110

Grocke SB, Cottrell E, de Silva S and Kelley KA. 2016. The role of crustal and eruptive processes versus source variations in controlling the oxidation state of iron in Central Andean magmas. Earth and Planetary Science Letters, 440: 92 – 104

Hao HD, Campbell IH, Park JW and Cooke DR. 2017. Platinum-group element geochemistry used to determine Cu and Au fertility in the Northparkes igneous suites, New South Wales, Australia. Geochimica et Cosmochimica Acta, 216: 372 – 392

Head E, Lanzirotti A, Newville M and Sutton S. 2018. Vanadium, sulfur, and iron valences in melt inclusions as a window into magmatic processes: A case study at Nyamuragira volcano, Africa. Geochimica et Cosmochimica Acta, 226: 149 – 173

Iacono-Marziano G, Gaillard F, Scaillet B, Polozov AG, Marecal V, Pirre M and Arndt NT. 2012. Extremely reducing conditions reached during basaltic intrusion in organic matter-bearing sediments. Earth and Planetary Science Letters, 357 – 358: 319 – 326

Jayasuriya KD, O'Neill HSC, Berry AJ and Campbell SJ. 2004. A Mössbauer study of the oxidation state of Fe in silicate melts. American Mineralogist, 89(11 – 12): 1597 – 1609

Jugo PJ. 2009. Sulfur content at sulfide saturation in oxidized magmas. Geology, 37(5): 415 – 418

Jugo PJ, Wilke M and Botcharnikov RE. 2010. Sulfur K-edge XANES analysis of natural and synthetic basaltic glasses: Implications for S speciation and S content as function of oxygen fugacity. Geochimica et Cosmochimica Acta, 74(20): 5926 – 5938

Karner JM, Papike JJ, Shearer CK, Mckay G, Le L and Burger P. 2007. Valence state partitioning of Cr and V between pyroxene-melt: Estimates of oxygen fugacity for martian basalt QUE 94201. American Mineralogist, 92(7): 1238 – 1241

Karner JM, Papike JJ, Sutton SR, Shearer CK, Burger P, McKay G and Le L. 2008. Valence state partitioning of V between pyroxene-melt: Effects of pyroxene and melt composition, and direct determination of V valence states by XANES. Application to Martian basalt QUE 94201 composition. Meteoritics & Planetary Science, 43(8): 1275 – 1285

Keays RR. 1995. The role of komatiitic and picritic magmatism and S-saturation in the formation of ore deposits. Lithos, 34(1 – 3): 1 – 18

Kelley KA and Cottrell E. 2012. The influence of magmatic differentiation on the oxidation state of Fe in a basaltic arc magma. Earth and Planetary Science Letters, 329 – 330: 109 – 121

Kress VC and Carmichael ISE. 1991. The compressibility of silicate liquids containing Fe_2O_3 and the effect of composition, temperature, oxygen fugacity and pressure on their redox states. Contributions to Mineralogy and Petrology, 108(1 – 2): 82 – 92

Lai SC and Zhou TZ. 1993. Study on the oxygen fugacity of magmas and its advance. Qinghai Geology, 2(2): 64 – 69 (in Chinese with English abstract)

Lanzirotti A, Dyar MD, Sutton S, Newville M, Head E, Carey CJ, McCanta M, Lee L, King PL and Jones J. 2018. Accurate predictions of microscale oxygen barometry in basaltic glasses using V K-edge X-ray absorption spectroscopy: A multivariate approach. American Mineralogist 103(8): 1282 – 1297.

Laubier M, Grove TL and Langmuir CH. 2014. Trace element mineral/melt partitioning for basaltic and basaltic andesitic melts: An experimental and laser ICP-MS study with application to the oxidation state of mantle source regions. Earth and Planetary Science Letters, 392: 265 – 278

Lazarov M, Woodland AB and Brey GP. 2009. Thermal state and redox conditions of the Kaapvaal mantle: A study of xenoliths from the Finsch mine, South Africa. Lithos, 112(Suppl. 2): 913 – 923

Lee CA. 1996. A review of mineralization in the bushveld complex and some other layered intrusions. In: Cawthorn RG (ed.). Layered Intrusions. Amsterdam: Elsevier, 103 – 145

Lee CTA, Leeman WP, Canil D and Li ZXA. 2005. Similar V/Sc systematics in MORB and arc basalts: Implications for the oxygen fugacities of their mantle source regions. Journal of Petrology, 46(11): 2313 – 2336

Lee CTA, Luffi P, Le Roux V, Dasgupta R, Albaréde F and Leeman WP. 2010. The redox state of arc mantle using Zn/Fe systematics. Nature, 468(7324): 681 – 685

Lee CTA, Luffi P, Chin EJ, Bouchet R, Dasgupta R, Morton DM, Le Roux V, Yin QZ and Jin D. 2012. Copper systematics in arc magmas and implications for crust-mantle differentiation. Science, 336(6077): 64 – 68

Li C and Ripley EM. 2011. The giant Jinchuan Ni-Cu-(PGE) deposit: Tectonic setting, magma evolution, ore genesis, and exploration implications. In: Li C and Ripley EM (eds.). Magmatic Ni-Cu and PGE Deposits: Geology, Geochemistry, and Genesis. Reviews in Economic Geology. Littleton: Society of Economic Geologists, 163 – 180

Li ZXA and Lee CTA. 2004. The constancy of upper mantle f_{O_2} through time inferred from V/Sc ratios in basalts. Earth and Planetary Science Letters, 228(3 – 4): 483 – 493

Lindsley DH and Frost BR. 1992. "Equilibria among Fe-Ti oxides, pyroxenes, olivine, and quartz; Part Ⅰ, Theory." American Mineralogist 77(9 – 10): 987 – 1003

Liu CQ, Li HP, Huang ZL and Su GL. 2001. A review of studies on oxygen fugacity of the earth mantle. Earth Science Frontiers, 8(3): 73 – 82 (in Chinese with English abstract)

Mallmann G and O'Neill HSC. 2009. The crystal/melt partitioning of V during mantle melting as a function of oxygen fugacity compared with some other elements (Al, P, Ca, Sc, Ti, Cr, Fe, Ga, Y, Zr and Nb). Journal of Petrology, 50(9): 1765 – 1794

Mallmann G and O'Neill HSC. 2013. Calibration of an empirical thermometer and oxybarometer based on the partitioning of Sc, Y and V between olivine and silicate melt. Journal of Petrology, 54(5): 933 – 949

Marks MAW, Scharrer M, Ladenburger S and Markl G. 2016. "Comment on "Apatite: A new redox proxy for silicic magmas?" [Geochimica et Cosmochimica Acta 132 (2014) 101 – 119]." Geochimica et Cosmochimica Acta 183: 267 – 270

Matjuschkin V, Blundy JD and Brooker RA. 2016. The effect of pressure on sulphur speciation in mid- to deep-crustal arc magmas and implications for the formation of porphyry copper deposits. Contributions to Mineralogy and Petrology, 171(7): 66

McCammon C and Kopylova MG. 2004. A redox profile of the Slave mantle and oxygen fugacity control in the cratonic mantle. Contributions to Mineralogy and Petrology, 148(1): 55 – 68

McCammon CA, Griffin WL, Shee SR and O'Neill HSC. 2001. Oxidation during metasomatism in ultramafic xenoliths from the Wesselton kimberlite, South Africa: Implications for the survival of diamond. Contributions to Mineralogy and Petrology, 141(3): 287 – 296

Miles AJ, Graham CM, Hawkesworth CJ, Gillespie MR, Hinton RW and Bromiley GD. 2014. Apatite: A new redox proxy for silicic magmas? Geochimica et Cosmochimica Acta, 132: 101 – 119

Molyneux TG. 1974. A geological investigation of the Bushveld Complex in Sekhukhuneland and part of the Steelpoort Valley. South African Journal of Geology, 77(3): 329 – 338

Morse SA. 1981. Kiglapait geochemistry Ⅳ: The major elements. Geochimica et Cosmochimica Acta, 45(3): 461 – 479

Morse SA. 2015. Kiglapait intrusion, labrador. In: Charlier B, Namur O, Latypov R and Tegner C (eds.). Layered Intrusions. Dordrecht: Springer, 589 – 648

Moussallam Y, Oppenheimer C, Scaillet B, Gaillard F, Kyle P, Peters N, Hartley M, Berlo K and Donovan A. 2014. Tracking the changing oxidation state of Erebus magmas, from mantle to surface, driven by magma ascent and degassing. Earth and Planetary Science Letters, 393: 200 – 209

Moussallam Y, Edmonds M, Scaillet B, Peters N, Gennaro E, Sides I and Oppenheimer C. 2016. The impact of degassing on the oxidation state of basaltic magmas: A case study of Kīlauea volcano. Earth and Planetary Science Letters, 450: 317 – 325

Mungall JE, Hanley JJ, Arndt NT and Debecdelievre A. 2006. Evidence from meimechites and other low-degree mantle melts for redox controls on mantle-crust fractionation of platinum-group elements. Proceedings of the National Academy of Sciences of the United States of America, 103(34): 12695 - 12700

Naldrett AJ. 2011. Fundamentals of magmatic sulfide deposits. In: Li C and Ripley EM (eds.). Magmatic Ni-Cu and PGE Deposits: Geology, Geochemistry and Genesis. Reviews in Economic Geology. Littleton: Society of Economic Geologists, 1 - 50

Naslund HR. 1983. The effect of oxygen fugacity on liquid immiscibility in iron-bearing silicate melts. American Journal of Science, 283(10): 1034 - 1059

O'Neill HSC, Berry AJ, McCammon CC, Jayasuriya KD, Campbell SJ and Foran G. 2006. An experimental determination of the effect of pressure on the $Fe^{3+}/\sum Fe$ ratio of an anhydrous silicate melt to 3.0GPa. American Mineralogist, 91(2 - 3): 404 - 412

O'Neill HSC and Wall VJ. 1987. The olivine-orthopyroxene-spinel oxygen geobarometer, the nickel precipitation curve, and the oxygen fugacity of the Earth's upper mantle. Journal of Petrology, 28(6): 1169 - 1191

Palme H and O'Neill HSC. 2014. Cosmochemical estimates of mantle composition. In: Holland HD and Turekian KK (ed.). Treatise on Geochemistry. 2nd Edition. Amsterdam: Elsevier, 1 - 39

Pang KN, Zhou MF, Lindsley D, Zhao DG and Malpas J. 2008. Origin of Fe-Ti oxide ores in mafic intrusions: Evidence from the panzhihua intrusion, SW China. Journal of Petrology, 49(2): 295 - 313

Papike JJ, Burger PV, Bell AS, Le L, Shearer CK, Sutton SR, Jones J and Newville M. 2013. Developing vanadium valence state oxybarometers (spinel-melt, olivine-melt, spinel-olivine) and V/(Cr + Al) partitioning (spinel-melt) for martian olivine-phyric basalts. American Mineralogist, 98(11 - 12): 2193 - 2196

Papike JJ, Simon SB, Burger PV, Bell AS, Shearer CK and Karner JM. 2016. Chromium, vanadium, and titanium valence systematics in Solar System pyroxene as a recorder of oxygen fugacity, planetary provenance, and processes. American Mineralogist, 101(4): 907 - 918

Park JW, Campbell IH, Kim J and Moon JW. 2015. The role of late sulfide saturation in the formation of a Cu- and Au-rich Magma: Insights from the platinum group element geochemistry of Niuatahi-Motutahi Lavas, Tonga Rear Arc. Journal of Petrology, 56(1): 59 - 81

Philpotts AR and Doyle CD. 1983. Effect of magma oxidation state on the extent of silicate liquid immiscibility in a tholeiitic basalt. American Journal of Science, 283(9): 967 - 986

Putirka KD. 2008. Thermometers and barometers for volcanic systems. Reviews in Mineralogy and Geochemistry, 69(1): 61 - 120

Putirka K. 2016. Rates and styles of planetary cooling on Earth, Moon, Mars, and Vesta, using new models for oxygen fugacity, ferric-ferrous ratios, olivine-liquid Fe-Mg exchange, and mantle potential temperature. American Mineralogist, 101(4): 819 - 840

Righter K, Sutton SR, Newville M, Le L, Schwandt CS, Uchida H, Lavina B and Downs RT. 2006. An experimental study of the oxidation state of vanadium in spinel and basaltic melt with implications for the origin of planetary basalt. American Mineralogist, 91(10): 1643 - 1656

Ripley EM and Li C. 2011. A review of conduit-related Ni-Cu-(PGE) sulfide mineralization at the Voiseys Bay Deposit, Labrador, and the Eagle Deposit, northern Michigan. In: Li C and Ripley EM (eds.). Magmatic Ni-Cu and PGE Deposits: Geology, Geochemistry, and Genesis. Reviews in Economic Geology. Littleton: Society of Economic Geologists, 181 - 197

Rowe MC, Kent AJR and Nielsen RL. 2009. Subduction influence on oxygen fugacity and trace and volatile elements in basalts across the cascade volcanic arc. Journal of Petrology, 50(1): 61 - 91

Shishkina T, Portnyagin M, Botcharnikov R, Almeev R, Simonyan A, Garbe-Schönberg D, Schuth S, Oeser M and Holtz F. 2018. Experimental calibration and implications of olivine-melt vanadium oxybarometry for hydrous basaltic arc magmas. American Mineralogist, 103(3): 369 - 383

Sisson TW. 2003. Native gold in a Hawaiian alkalic magma. Economic Geology, 98(3): 643 - 648

Smythe DJ and Brenan JM. 2016. Magmatic oxygen fugacity estimated using zircon-melt partitioning of cerium. Earth and Planetary Science Letters, 453: 260 - 266

Song XY, Qi HW, Hu RZ, Chen LM, Yu SY and Zhang JF. 2013. Formation of thick stratiform Fe-Ti oxide layers in layered intrusion and frequent replenishment of fractionated mafic magma: Evidence from the Panzhihua intrusion, SW China. Geochemistry, Geophysics, Geosystems, 14(3): 712 - 732

Song XY, Yi JN, Chen LM, She YW, Liu CZ, Dang XY, Yang QA and Wu SK. 2016. The giant Xiarihamu Ni-Co sulfide deposit in the East Kunlun orogenic belt, Northern Tibet Plateau, China. Economic Geology, 111(1): 29 - 55

Sun WD, Arculus RJ, Kamenetsky VS and Binns RA. 2004. Release of gold-bearing fluids in convergent margin magmas prompted by magnetite crystallization. Nature, 431(7011): 975 - 978

Sutton SR, Karner J, Papike J, Delaney JS, Shearer C, Newville M, Eng P, Rivers M and Dyar MD. 2005. Vanadium K edge XANES of synthetic and natural basaltic glasses and application to microscale oxygen barometry. Geochimica et Cosmochimica Acta, 69(9): 2333 - 2348

Tegner C and Cawthorn RG. 2010. Iron in plagioclase in the Bushveld and Skaergaard intrusions: Implications for iron contents in evolving basic magmas. Contributions to Mineralogy and Petrology, 159(5): 719 - 730

Thakurta J, Ripley EM and Li C. 2008. Geochemical constraints on the origin of sulfide mineralization in the Duke Island Complex, southeastern Alaska. Geochemistry, Geophysics, Geosystems, 9(7): Q07003

Tomkins AG, Rebryna KC, Weinberg RF and Schaefer BF. 2012. Magmatic sulfide formation by reduction of oxidized arc basalt. Journal of Petrology, 53(8): 1537 - 1567

Toplis MJ and Carroll MR. 1995. An experimental study of the influence of oxygen fugacity on Fe-Ti oxide stability, phase relations, and mineral-melt equilibria in ferro-basaltic systems. Journal of Petrology, 36(5): 1137 - 1170

Toplis MJ and Corgne A. 2002. An experimental study of element partitioning between magnetite, clinopyroxene and iron-bearing silicate liquids with particular emphasis on vanadium. Contributions to Mineralogy and Petrology, 144(1): 22 - 37

Trail D, Bruce Watson E and Tailby ND. 2012. Ce and Eu anomalies in zircon as proxies for the oxidation state of magmas. Geochimica et Cosmochimica Acta, 97: 70 - 87

Vigouroux N, Wallace PJ and Kent AJR. 2008. Volatiles in high-K magmas from the western trans-Mexican volcanic belt: Evidence for fluid fluxing and extreme enrichment of the mantle wedge by subduction processes. Journal of Petrology, 49(9): 1589 - 1618

Wang Y, Wang K, Xing CM, Wei B, Dong H and Cao YH. 2017. Metallogenic diversity related to the late Middle Permian Emeishan large igneous province. Bulletin of Mineralogy, Petrology and Geochemistry, 36(3): 404 - 417 (in Chinese with English abstract)

Wijbrans CH, Klemme S, Berndt J and Vollmer C. 2015. Experimental determination of trace element partition coefficients between spinel and silicate melt: The influence of chemical composition and oxygen fugacity. Contributions to Mineralogy and Petrology, 169(4): 45

Wood BJ, Bryndzia LT and Johnson KE. 1990. Mantle oxidation state and its relationship to tectonic environment and fluid speciation. Science, 248(4953): 337 - 345

Wood BJ. 1991. Oxygen barometry of spinel peridotites. Reviews in Mineralogy and Geochemistry, 25(1): 417 - 432

Woodland AB, Kornprobst J, McPherson E, Bodinier JL and Menzies MA. 1996. Metasomatic interactions in the lithospheric mantle: Petrologic evidence from the Lherz massif, French Pyrenees. Chemical Geology, 134(1 - 3): 83 - 112

Woodland AB and Koch M. 2003. Variation in oxygen fugacity with depth

in the upper mantle beneath the Kaapvaal craton, Southern Africa. Earth and Planetary Science Letters, 214(1-2): 295-310

Xu YG, Wang Y, Wei X and He B. 2013. Mantle plume-related mineralization and their principal controlling factors. Acta Petrologica Sinica, 29(10): 3307-3322 (in Chinese with English abstract)

Yu XH. 1990. An introduction to research on mantle redox state and its oxygen fugacity. Geological Science and Technology Information, 9(4): 25-29 (in Chinese with English abstract)

Zhang HL, Hirschmann MM, Cottrell E, Newville M and Lanzirotti A. 2016. Structural environment of iron and accurate determination of $Fe^{3+}/\sum Fe$ ratios in andesitic glasses by XANES and Mössbauer spectroscopy. Chemical Geology, 428: 48-58

Zhang HL, Hirschmann MM, Cottrell E and Withers AC. 2017. Effect of pressure on $Fe^{3+}/\sum Fe$ ratio in a mafic magma and consequences for magma ocean redox gradients. Geochimica et Cosmochimica Acta, 204: 83-103

Zhong H, Zhou XH, Zhou MF, Sun M and Liu BG. 2002. Platinum-group element geochemistry of the Hongge Fe-V-Ti deposit in the Pan-Xi area, southwestern China. Mineralium Deposita, 37(2): 226-239

Zhong H, Hu RZ, Wilson AH and Zhu WG. 2005. Review of the link between the Hongge layered intrusion and Emeishan flood basalts, Southwest China. International Geology Review, 47(9): 971-985

附中文参考文献

赖绍聪, 周天祯. 1993. **岩浆氧逸度及其研究进展**. **青海地质**, 2(2): 64-69

刘丛强, 李和平, 黄智龙, 苏根利. 2001. **地幔氧逸度的研究进展**. **地学前缘**, 8(3): 73-82

王焰, 王坤, 邢长明, 魏博, 董欢, 曹永华. 2017. **二叠纪峨眉山地幔柱岩浆成矿作用的多样性**. **矿物岩石地球化学通报**, 36(3): 404-417

徐义刚, 王焰, 位荀, 何斌. 2013. **与地幔柱有关的成矿作用及其主控因素**. **岩石学报**, 29(10): 3307-3322

喻学惠. 1990. **地幔氧化状态和氧逸度简介**. **地质科技情报**, 9(4): 25-29